EUROPEAN ORGANIZATION FOR NUCLEAR RESEARCH

CERN-PPE/95-41
March 31, 1995

Tests of QED at LEP Energies using $e^+e^- \to \gamma\gamma(\gamma)$ and $e^+e^- \to \ell^+\ell^-\gamma\gamma$

The L3 Collaboration

Abstract

Total and differential cross sections for the process $e^+e^- \to \gamma\gamma(\gamma)$, and the total cross section for the process $e^+e^- \to \gamma\gamma\gamma$, are measured at energies around 91 GeV using the data collected with the L3 detector from 1991 to 1993. We set lower limits, at 95% CL, on a contact interaction energy scale parameter $\Lambda > 602$ GeV, on the mass of an excited electron $m_{e^*} >$146 GeV and on the QED cut-off parameters $\Lambda_+ >$ 149 GeV and $\Lambda_- > 143$ GeV. Upper limits are also set on the branching fractions of Z decaying into $\gamma\gamma$, $\pi^\circ\gamma$ and $\eta\gamma$ of 5.2×10^{-5}, 5.2×10^{-5} and 7.6×10^{-5} respectively. The reactions $e^+e^- \to \ell^+\ell^-(n\gamma)$ $(\ell = e, \mu, \tau)$ are studied using the data collected from 1990 to 1994. The data are consistent with the QED expectations.

(Submitted to Phys. Lett. B)

Introduction

The reaction $e^+e^- \rightarrow \gamma\gamma(\gamma)$ [1)] is an ideal process to test QED at the Z resonance. The present statistics enables us to compare the data with the QED prediction up to $O(\alpha^3)$. The degree of agreement between QED and the data can be used to constrain different models with QED breakdown effects.

The forbidden decay $Z \rightarrow \gamma\gamma$ and the rare decays $Z \rightarrow \pi^\circ\gamma$ and $Z \rightarrow \eta\gamma$ [1] would have the same experimental signatures as the process $e^+e^- \rightarrow \gamma\gamma$. The measurement of the total cross section as a function of center of mass energy, $\sqrt{s}$, can be used to set limits on these processes.

Similar analyses have been carried out earlier at LEP [2]. Since our previous publication on this subject, the integrated luminosity has increased by about a factor of five. The higher statistics enables us to test QED and to set improved limits on the various scale parameters. The total cross section for the process $e^+e^- \rightarrow \gamma\gamma\gamma$ is also measured for the case where the photons are well separated [3]. New limits on the branching fraction for the Z decays with photonic final states are obtained.

Compared to our previous publication [4] on the analysis of the reactions $e^+e^- \rightarrow \ell^+\ell^-(n\gamma)$, an increase of integrated luminosity by about a factor of four enables us to test QED via these processes and to clarify the open question about the origin of the four events with high $\gamma\gamma$ invariant mass. These reactions have also been investigated by other LEP experiments [5].

The L3 Detector

The L3 detector is described in detail in Ref. [6]. The main components of the detector relevant to the analysis are a central tracking chamber, a Z-chamber, forward-backward tracking chambers, a high resolution electromagnetic calorimeter (ECAL) composed of bismuth germanium oxide (BGO) crystals with a barrel region ($42^\circ < \theta < 138^\circ$) and two endcaps ($11^\circ < \theta < 37^\circ$ and $143^\circ < \theta < 169^\circ$), a ring of scintillation counters, a sampling hadron calorimeter with uranium absorbers and proportional wire chamber readout, and a high precision muon spectrometer. Forward BGO arrays on either side of the detector measure the luminosity by detecting small-angle Bhabha events. All subdetectors are located in a 12m diameter magnet which provides a uniform field of 0.5 T along the beam direction. The energy and angular resolution for electrons and photons with energies above 1 GeV are better than 2% and 0.5°, respectively.

Event Selection

In order to select events with two or more electromagnetic showers with polar angles in the range $14^\circ < \theta < 166^\circ$, the following cuts are applied:

(1) the number of showers with energy above 2.0 GeV in the ECAL must be at least 2 and less than 8;

(2) the total energy deposited in the ECAL must be higher than $0.7\sqrt{s}$;

(3) the shower profiles must be consistent with that of an electron or a photon;

(4) the acollinearity angle between the two most energetic showers is required to be less than 40°.

[1]The photon within parentheses indicates the possible presence of a third photon.

After these cuts the sample contains mostly Bhabha events and $e^+e^- \to \gamma\gamma(\gamma)$ events. The Bhabha events are rejected if:

(5) there is a track in the central tracking chamber, or there are hits in the forward-backward tracking chambers associated with either of the two most energetic showers in the ECAL.

In total, 1882 $e^+e^- \to \gamma\gamma(\gamma)$ events are selected in the data taking period from 1991 to 1993 corresponding to an integrated luminosity of 64.6 pb^{-1} in the center of mass energy range 88.5–93.7 GeV. Using the Bhabha data sample to estimate the tracking chamber veto efficiency for charged particles, the contamination from Bhabha events is estimated to be less than 0.5%.

To select $e^+e^- \to \gamma\gamma\gamma$ events where all three photons are hard and well separated, the following two cuts are applied in addition to cuts 1, 2, 3 and 5:

(6) there must be at least three showers in the ECAL separated from each other by at least 15° and the energy of the third most energetic shower must be greater than 5 GeV;

(7) the sum of the angles in space between the three showers has to exceed 350°.

A total of 52 $e^+e^- \to \gamma\gamma\gamma$ events are selected in the data sample.

The selection criteria for $e^+e^- \to \ell^+\ell^-(n\gamma)$ (n =1 or 2) events are the same as in our previous publication [4]. Briefly they are as follows: electrons are selected within the fiducial region defined by $|\cos\theta| < 0.74$ and with energies above 3.0 GeV; muons are selected using the muon spectrometer with a minimum momentum requirement of 3.0 GeV; taus are identified within $|\cos\theta| < 0.74$ via their distinctive one and three-prong decays; photons are required to be within $|\cos\theta| < 0.9$ and to have energies above 1.0 GeV; their isolation angles from the electrons, muons or taus should be greater than 8°, 5° and 15° respectively. A total of 689 $e^+e^- \to \ell^+\ell^-\gamma\gamma$ events are selected in the data taking period from 1990 to 1994, corresponding to an integrated luminosity of 114 pb^{-1}.

$e^+e^- \to \gamma\gamma(\gamma)$ Results

In order to measure the total and differential cross sections for the reaction $e^+e^- \to \gamma\gamma(\gamma)$, a QED Monte Carlo generator [7] is used to calculate the selection efficiency. This generator includes soft and hard bremsstrahlung, and virtual photon corrections up to $O(\alpha^3)$. The generated events are passed through the L3 simulation and reconstruction programs. The QED event selection efficiency is $(89 \pm 1)\%$ in the region $|\cos\theta| \leq 0.71$, $(70 \pm 1)\%$ in the region $0.82 < |\cos\theta| \leq 0.94$ and $(15 \pm 2)\%$ in the region $0.94 < |\cos\theta| \leq 0.97$. The trigger efficiency is estimated to be 99.7%.

Figs. 1a, 1b and 1c show comparisons of the photon energy spectra between the data and the Monte Carlo (normalized to the integrated luminosity) after cuts 1–5. Fig. 1d shows the comparison of the acollinearity angle, ζ, distribution of the two most energetic photons with the same cuts applied. Good agreement is observed between the data and the Monte Carlo. The total cross sections for $e^+e^- \to \gamma\gamma(\gamma)$ measured at each $\sqrt{s}$ point are shown in Fig. 2a. The cross section at $\sqrt{s} = 91.2$ GeV is 55.3±1.5 pb. The measurement of the total cross section for $e^+e^- \to \gamma\gamma\gamma$ is shown in Fig. 2b for the three energies with highest luminosity. Table 1 lists the measured and radiatively corrected $e^+e^- \to \gamma\gamma(\gamma)$ differential cross sections and the number of events per angular bin. $|\cos\theta|$ is defined as the average of $|\cos\theta_1|$ and $|\cos\theta_2|$ with θ_1 and θ_2 as the polar angles of the first and second most energetic showers respectively. The off-peak data are scaled to the peak energy, $\sqrt{s}$= 91.2 GeV, because the angular distribution for the differential cross section is energy independent and they have small small statistics. The systematic error is estimated to be 2.7%, mainly originating from the detector efficiency calculation. A graphical representation of the differential cross sections given in Table 1 together with the QED Born level (lowest order) prediction is shown in Fig. 3a. Fig. 3b shows the same cross sections normalized to the Born level prediction. The comparison of the data with the QED radiatively corrected expectation leads to a χ^2 = 9 for 17 degrees of freedom. This shows that the measured differential cross section agrees with the QED prediction including radiative corrections up to $O(\alpha^3)$.

$\mid\cos\theta\mid$	$N_{\gamma\gamma(\gamma)}$ (1991-1993)	$\left(\frac{d\sigma_{meas}}{d\Omega_{\gamma\gamma(\gamma)}}\right)$ (pb/sr) (1991-1993)	$\left(\frac{d\sigma_{QED}}{d\Omega_{\gamma\gamma(\gamma)}}\right)$ (pb/sr)
0.027	37	1.8 $\pm$ 0.3	1.76
0.082	47	2.3 $\pm$ 0.3	2.29
0.135	58	2.8 $\pm$ 0.4	2.68
0.190	51	2.5 $\pm$ 0.3	2.98
0.244	61	3.4 $\pm$ 0.4	3.21
0.299	61	3.3 $\pm$ 0.4	3.43
0.353	71	3.9 $\pm$ 0.5	3.64
0.408	64	3.5 $\pm$ 0.4	3.89
0.463	87	4.4 $\pm$ 0.5	4.20
0.517	88	4.4 $\pm$ 0.5	4.61
0.572	107	5.4 $\pm$ 0.5	5.17
0.627	132	6.7 $\pm$ 0.6	5.95
0.681	122	6.6 $\pm$ 0.6	7.07
0.844	222	15.7 $\pm$ 1.0	16.01
0.890	300	23.2 $\pm$ 1.3	23.89
0.926	268	40.5 $\pm$ 2.5	37.58
0.958	106	74.0 $\pm$ 7.2	68.68

Table 1: Number of observed events and differential cross sections for the process $e^+e^- \to \gamma\gamma(\gamma)$ as a function of $\mid\cos\theta\mid$. The errors are statistical only.

The agreement between the data and the QED predictions can be used to constrain various models with deviation from QED predictions. A possible deviation from QED may arise from the effective interactions with non-standard $e^+e^-\gamma$ couplings and $e^+e^-\gamma\gamma$ contact terms [8]. We will refer to this as the "contact interaction assumption". Another possibility would be the existence of an excited electron, e^*, with mass m_{e^*}. If such an electron exists, it could couple to an electron and a photon via a magnetic interaction and replace the virtual electron in the QED process [9,10]. A convenient and simple way of quantifying QED deviations is the introduction of QED cut-off parameters, Λ_+ and Λ_- [10].

For the above cases, it is possible to express the differential cross sections in a form similar to the known QED differential cross section $(d\sigma/d\Omega)_{\rm QED}$ by adding a deviation term, $\delta_{\rm new}$:

$$(d\sigma/d\Omega) = (d\sigma/d\Omega)_{\rm QED}\,(1 + \delta_{\rm new}) \qquad (1)$$

For the contact interaction assumption we use $\delta_{\rm new} = s^2/(2\alpha)\ \left(1/\Lambda^4 + 1/\tilde{\Lambda}^4\right)\ (1-\cos^2\theta)$, which is the most stringent case [8], with Λ and $\tilde{\Lambda}$ as energy scale parameters. For the excited electron assumption, the deviation can be written in terms of the QED cut-off parameters as $\delta_{\rm new} \cong \pm s^2/2\ \left(1/\Lambda_\pm^4\right)\ (1-\cos^2\theta)$. In the $s/m_{e^*}^2 << 1$ limit, the excited electron mass can be written as $m_{e^*}^2 = \lambda \cdot \Lambda_+^2$, where λ is a coupling constant. The full expression for m_{e^*} can be found in Ref. [10].

In Eqn. 1 the cross section for the contact interaction or for the excited electron is calculated at the Born level. To estimate the deviation from QED, we replace the QED Born level cross section with the QED cross section corrected for radiative effects up to $O(\alpha^3)$:

$$(d\sigma/d\Omega) = \ (d\sigma/d\Omega)_{\rm QED}^{O(\alpha^3)}\,(1\ +\ \delta_{\rm new})\,.$$

To set lower limits on the parameters in $\delta_{\rm new}$, the unbinned and the optimized binning maximum likelihood methods [11] are used. As both methods give very similar results, only the unbinned method is described here. The likelihood function is chosen as:

$$L(\Lambda_{\rm p}) \ = \ \frac{1}{\sqrt{2\pi\sigma^2}}\ \exp\left(\frac{-(N_{\rm obs}-N_{\rm theo}(\Lambda_{\rm p}))^2}{2\sigma^2}\right)\ \prod_{i=1}^{N_{\rm obs}} P(\theta_i;\Lambda_{\rm p}) \qquad (2)$$

where $\Lambda_{\rm p}$ stands for the parameter Λ, m_{e^*} or $\Lambda_\pm$; $N_{\rm obs}$ is the total number of observed events; $N_{\rm theo}(\Lambda_{\rm p})$ is the total number of expected events and $P(\theta_i;\Lambda_{\rm p})$ is the event probability density. The term before the product in Eqn.2 corresponds to an overall normalization constraint. The error σ includes the statistical and the systematic errors added in quadrature. For the hypothesis of contact interaction the scale Λ is varied for the assumption $\Lambda \equiv \tilde{\Lambda}$ [8]. To set a limit on the mass of the excited electron, m_{e^*}, the full expression for the differential cross section given in Ref. [10] is used under the assumption that the coupling constant $\lambda = 1$. At 95% CL we find $\Lambda > 602$ GeV, $m_{e^*} > 146$ GeV, $\Lambda_+ > 149$ GeV, and $\Lambda_- > 143$ GeV. In order to calculate the limits we use a Gaussian distribution which contains the full positive parameter space and renormalize this area to one [12]. Fig. 4 shows the ratio of the measured to the radiatively corrected QED differential cross section as a function of $|\cos\theta|$. The curves illustrate the effects of Λ, Λ_+ and Λ_- on the QED prediction.

Other deviations from QED could come from the forbidden decay $Z\rightarrow\gamma\gamma$, or the rare decays $Z\rightarrow\pi^\circ\gamma$ and $Z\rightarrow\eta\gamma$ [1]. At high energies, the two photons from the π° or η are too close to be separated and are seen as a single shower in the ECAL. All three reactions leave the same two photon signature in the detector as the QED reaction apart from the angular distribution of the photons.

The Born level cross section at the Z pole for $Z\rightarrow X$ is given by:

$$\sigma_{\rm pole} \ = \ \frac{12\pi}{m_{\rm Z}^2}\ \frac{\Gamma_{\rm ee}\,\Gamma_{\rm X}}{\Gamma_{\rm Z}^2}$$

where $\Gamma_{\rm X}$ is the width of the rare decay mode under consideration, $\Gamma_{\rm ee}$ is the electronic decay width, and $m_{\rm Z}$ and $\Gamma_{\rm Z}$ are the mass and the total width of the Z respectively. The variation of the cross section with the center of mass energy is given by a Breit-Wigner ansatz:

$$\sigma(s) \ = \ \sigma_{\rm pole}\ \frac{s\Gamma_{\rm Z}^2}{(s-m_{\rm Z}^2)^2\ +\ (s\Gamma_{\rm Z}/m_{\rm Z})^2}$$

For $\Gamma_{\rm ee}$, $\Gamma_{\rm Z}$ and $m_{\rm Z}$ we use our measured values [13]. The selection efficiencies in the angular range $14^\circ < \theta < 166^\circ$ for these decays are estimated using Monte Carlo events with an angular distribution of $(1 + \cos^2\theta)$ [1]. This leads to an efficiency of $(73 \pm 2)\%$ for Z$\rightarrow \gamma\gamma$ and Z$\rightarrow \pi^\circ\gamma$ events and $(52 \pm 2)\%$ for Z$\rightarrow \eta\gamma$ events (the η neutral decay fraction is 71%). The likelihood function used to calculate the limits for the rare decay width Γ_X is

$$L(\Gamma_X) = \prod_{i=1}^{7} P(N_i, N_{\mathrm{theo}}(\Gamma_X))$$

where P is the Poisson distribution function, N_i the number of observed events at an energy point, i, and N_{theo} the number of expected events from QED plus the contribution from the Z$\rightarrow X$ decay. With this likelihood function the 95% CL upper limits obtained are:

$$\Gamma(\mathrm{Z}\rightarrow \pi^\circ\gamma/\gamma\gamma) < 0.13 \text{ MeV or BR}(\mathrm{Z}\rightarrow \pi^\circ\gamma/\gamma\gamma) < 5.2 \times 10^{-5},$$

$$\Gamma(\mathrm{Z}\rightarrow \eta\gamma) < 0.19 \text{ MeV or BR}(\mathrm{Z}\rightarrow \eta\gamma) < 7.6 \times 10^{-5}.$$

The above limits on Γ_X are used to estimate the possible deviations from QED as shown in Fig. 2a. The curve for the decay Z$\rightarrow \eta\gamma$ is separated from that for Z$\rightarrow \pi^\circ\gamma$ and Z$\rightarrow \gamma\gamma$ due to the η neutral decay branching fraction.

$\mathbf{e^+e^- \rightarrow \ell^+\ell^-(n\gamma)}$ Results

The accumulated high luminosity makes it possible to test QED via the reaction $e^+e^- \rightarrow \ell^+\ell^-(n\gamma)$. There exist several QED calculations and Monte Carlo simulations for this process. The YFS approach [14] and the matrix element calculation approach [15] predict the same cross section for hard isolated photon production. The agreement between the two approaches for the $\gamma\gamma$ invariant mass distribution is better than 10% [16]. As in our previous analysis, the Monte Carlo program YFS3 [17] is used for the QED calculation. Table 2 gives a comparison between the data and the Monte Carlo expectation for the number of $\ell^+\ell^-(n\gamma)$ events with $n \geq 1$ and $n \geq 2$.

	1990 to 1994 data				Monte Carlo expectation			
n	ee $(n\gamma)$	$\mu\mu$ $(n\gamma)$	$\tau\tau$ $(n\gamma)$	$\ell\ell$ $(n\gamma)$	ee $(n\gamma)$	$\mu\mu$ $(n\gamma)$	$\tau\tau$ $(n\gamma)$	$\ell\ell$ $(n\gamma)$
$n \geq 1$	7138	6720	4262	18120	6857	6925	4680	18462
$n \geq 2$	268	286	135	689	238	278	125	641

Table 2: Number of $e^+e^- \rightarrow \ell^+\ell^-(n\gamma)$ events compared to Monte Carlo expectations.

Fig. 5 shows the $\gamma\gamma$ invariant mass distribution. Reasonable agreement between the data and the QED prediction is observed. At lower mass, the discrepancies originate mainly from the use of a generator level Monte Carlo, with the directions and energies of the final state particles smeared according to our detector resolutions. Using the YFS3 program, we calculate a probability of 25% to observe more than 5 events with a $\gamma\gamma$ invariant mass above 50 GeV with 4 of them within an interval of 5 GeV.

Conclusions

The measurements of total and differential cross sections for $e^+e^- \rightarrow \gamma\gamma(\gamma)$ are well described by QED. The measured total cross section for the process $e^+e^- \rightarrow \gamma\gamma\gamma$ is in good agreement with the QED prediction. At 95% CL, we set the following lower limits: the contact interaction energy scale parameter $\Lambda > 602$ GeV; the excited electron mass $m_{e^*} >$146 GeV; and the QED cut-off parameters $\Lambda_+ > 149$ GeV and $\Lambda_- > 143$ GeV. Upper limits are set, at 95% CL, on the branching fractions of Z decaying into $\gamma\gamma$, $\pi^\circ\gamma$, and $\eta\gamma$ of 5.2×10^{-5}, 5.2×10^{-5} and 7.6×10^{-5} respectively. The increased statistics indicates that there is no further evidence for a high $\gamma\gamma$ mass anomaly in the $\ell\ell\gamma\gamma$ channel.

Acknowledgements

We wish to express our gratitude to the CERN accelerator divisions for the excellent performance of the LEP machine. We acknowledge the effort of all engineers and technicians who have participated in the construction and maintenance of the experiment.

References

[1] M. Jacob, T. T. Wu, Phys. Lett. **B232** (1989) 529;
G. B. West, Mod. Phys. Lett. **A5** No. 27 (1990) 2281;
S. Ghosh, D. Chatterjee, Mod. Phys. Lett. **A5** No. 19 (1990) 1493;
E.W.N. Glover, I.J. van der Bij, in *"Z physics at LEP 1"*, eds. G. Altarelli *et al.*, CERN Report 89-08 vol. 2, 1.

[2] OPAL Collab., M. Z. Akrawy *et al.*, Phys. Lett. **B257** (1991) 531;
L3 Collab., O. Adriani *et al.*, Phys. Lett. **B288** (1992) 404;
ALEPH Collab., D. Decamp, *et al.*, Phys. Rep. **216** (1992) 253;
DELPHI Collab., P. Abreu, *et al.*, Phys. Lett. **B327**(1994) 386.

[3] L3 Collab., M.Acciarri *et al.*, CERN-PPE/94-186 (1994) (CERN Preprint).

[4] L3 Collab., O.Adriani *et al.*, Phys. Lett. **B295** (1992) 337.

[5] ALEPH Collab., D. Buskulic *et al.*, Phys. Lett. **B308** (1993) 425;
OPAL Collab., P.D. Acton *et al.*, Phys. Lett. **B311** (1993) 391.

[6] L3 Collab., B. Adeva *et al.*, Nucl. Instr. and Meth. **A289** (1990) 35;
O. Adriani *et al.*, Phys. Rep. **236** (1993) 1.

[7] F.A. Berends and R. Kleiss, Nucl. Phys. **B186** (1981) 22.

[8] O. J. P. Eboli *et al.*, Phys. Lett. **B271** (1991) 274.

[9] F.E. Low, Phys. Rev. Lett. **14** (1965) 238;
R. P. Feynman, Phys. Rev. Lett. **74** (1948) 939;
F. M. Renard, Phys. Lett. **B116** (1982) 264;
S. Drell, Ann. Phys. (N.Y.) **4** (1958) 75.

[10] A. Litke, Harvard Univ., Ph.D Thesis (1970) unpublished.

[11] W. T. Eadie *et al.*, *"Statistical Methods in Experimental Physics"*, North Holland (1971) 268.

[12] L. Montanet *et al.*, Review of Particle Properties, Phys. Rev. **D50** (1994) 1278.

[13] L3 Collab., M.Acciarri *et al.*, Z. Phys. **C62** (1994) 551.

[14] D.R.Yennie, S.C.Frautschi and H.Suura, Ann. Phys. **13** (1961) 379.

[15] W.J.Stirling, Phys. Lett. **B271** (1991) 261;
D.J.Summers, DTP/92/76 (1992) (Durham Preprint) ;
M.Martinez and R.Miquel, CERN-PPE/92-211 (1992) (CERN Preprint).

[16] K.Riles, UM-HE-92-36 (1992) (Univ. of Michigan Preprint).

[17] S.Jadach and B.F.L.Ward, Phys. Lett. **B274** (1992) 470.

The L3 Collaboration:

M.Acciarri,[26] A.Adam,[43] O.Adriani,[16] M.Aguilar-Benitez,[25] S.Ahlen,[10] B.Alpat,[33] J.Alcaraz,[25] J.Allaby,[17] A.Aloisio,[28] G.Alverson,[11] M.G.Alviggi,[28] G.Ambrosi,[33] Q.An,[18] H.Anderhub,[46] V.P.Andreev,[37] T.Angelescu,[12] D.Antreasyan,[8] A.Arefiev,[27] T.Azemoon,[3] T.Aziz,[9] P.V.K.S.Baba,[18] P.Bagnaia,[36,17] L.Baksay,[42] R.C.Ball,[3] S.Banerjee,[9] K.Banicz,[43] R.Barillère,[17] L.Barone,[36] P.Bartalini,[33] A.Baschirotto,[26] M.Basile,[8] R.Battiston,[33] A.Bay,[22] F.Becattini,[16] U.Becker,[15] F.Behner,[46] Gy.L.Bencze,[13] J.Berdugo,[25] P.Berges,[15] B.Bertucci,[17] B.L.Betev,[46] M.Biasini,[33] A.Biland,[46] G.M.Bilei[33] R.Bizzarri,[36] J.J.Blaising,[17] G.J.Bobbink,[2] R.Bock,[1] A.Böhm,[1] B.Borgia,[36] A.Boucham,[4] D.Bourilkov,[46] M.Bourquin,[19] D.Boutigny,[4] B.Bouwens,[2] E.Brambilla,[15] J.G.Branson,[38] V.Brigljevic,[46] I.C.Brock,[34] A.Bujak,[43] J.D.Burger,[15] W.J.Burger,[19] C.Burgos,[25] J.Busenitz,[42] A.Buytenhuijs,[30] X.D.Cai,[18] M.Capell,[15] G.Cara Romeo,[8] M.Caria,[33] G.Carlino,[28] A.M.Cartacci,[16] J.Casaus,[25] G.Castellini,[16] R.Castello,[26] N.Cavallo,[28] C.Cecchi,[19] M.Cerrada,[25] F.Cesaroni,[36] M.Chamizo,[25] A.Chan,[48] Y.H.Chang,[48] U.K.Chaturvedi,[18] M.Chemarin,[24] A.Chen,[48] C.Chen,[6] G.Chen,[6] G.M.Chen,[6] H.F.Chen,[20] H.S.Chen,[6] M.Chen,[15] G.Chiefari,[28] C.Y.Chien,[5] M.T.Choi,[41] L.Cifarelli,[8] F.Cindolo,[8] C.Civinini,[16] I.Clare,[15] R.Clare,[15] T.E.Coan,[23] H.O.Cohn,[31] G.Coignet,[4] N.Colino,[17] V.Commichau,[1] S.Costantini,[36] F.Cotorobai,[12] B.de la Cruz,[25] X.T.Cui,[18] X.Y.Cui,[18] T.S.Dai,[15] R.D'Alessandro,[16] R.de Asmundis,[28] H.De Boeck,[30] A.Degré,[4] K.Deiters,[44] E.Dénes,[13] P.Denes,[35] F.DeNotaristefani,[36] D.DiBitonto,[42] M.Diemoz,[36] C.Dionisi,[36] M.Dittmar,[46] A.Dominguez,[38] A.Doria,[28] I.Dorne,[4] M.T.Dova,[18,♯] E.Drago,[28] D.Duchesneau,[17] P.Duinker,[2] I.Duran,[39] S.Dutta,[9] S.Easo,[33] Yu.Efremenko,[31] H.El Mamouni,[24] A.Engler,[34] F.J.Eppling,[15] F.C.Erné,[2] J.P.Ernenwein,[24] P.Extermann,[19] R.Fabbretti,[44] M.Fabre,[44] R.Faccini,[36] S.Falciano,[36] A.Favara,[16] J.Fay,[24] M.Felcini,[46] T.Ferguson,[34] D.Fernandez,[25] G.Fernandez,[25] F.Ferroni,[36] H.Fesefeldt,[1] E.Fiandrini,[33] J.H.Field,[19] F.Filthaut,[34] P.H.Fisher,[15] G.Forconi,[15] L.Fredj,[19] K.Freudenreich,[46] M.Gailloud,[22] Yu.Galaktionov,[27,15] S.N.Ganguli,[9] P.Garcia-Abia,[25] S.S.Gau,[11] S.Gentile,[36] J.Gerald,[5] N.Gheordanescu,[12] S.Giagu,[36] S.Goldfarb,[22] J.Goldstein,[10] Z.F.Gong,[20] E.Gonzalez,[25] A.Gougas,[5] D.Goujon,[19] G.Gratta,[32] M.W.Gruenewald,[7] C.Gu,[18] M.Guanziroli,[18] V.K.Gupta,[35] A.Gurtu,[9] H.R.Gustafson,[3] L.J.Gutay,[43] B.Hartmann,[1] A.Hasan,[29] J.T.He,[6] T.Hebbeker,[7] A.Hervé,[17] K.Hilgers,[1] W.C.van Hoek,[30] H.Hofer,[46] H.Hoorani,[19] S.R.Hou,[48] G.Hu,[18] M.M.Ilyas,[18] V.Innocente,[17] H.Janssen,[4] B.N.Jin,[6] L.W.Jones,[3] P.de Jong,[15] I.Josa-Mutuberria,[25] A.Kasser,[22] R.A.Khan,[18] Yu.Kamyshkov,[31] P.Kapinos,[45] J.S.Kapustinsky,[23] Y.Karyotakis,[4] M.Kaur,[18] S.Khokhar,[18] M.N.Kienzle-Focacci,[19] D.Kim,[5] J.K.Kim,[41] S.C.Kim,[41] Y.G.Kim,[41] W.W.Kinnison,[23] A.Kirkby,[32] D.Kirkby,[32] J.Kirkby,[17] S.Kirsch,[45] W.Kittel,[30] A.Klimentov,[15,27] A.C.König,[30] E.Koffeman,[2] O.Kornadt,[1] V.Koutsenko,[15,27] A.Koulbardis,[37] R.W.Kraemer,[34] T.Kramer,[15] W.Krenz,[1] H.Kuijten,[30] A.Kunin,[15,27] P.Ladron de Guevara,[25] G.Landi,[16] C.Lapoint,[15] K.Lassila-Perini,[46] P.Laurikainen,[21] M.Lebeau,[17] A.Lebedev,[15] P.Lebrun,[24] P.Lecomte,[46] J.Lecoq,[4] P.Lecoq,[17] P.Le Coultre,[46] J.S.Lee,[41] K.Y.Lee,[41] C.Leggett,[3] J.M.Le Goff,[17] R.Leiste,[45] M.Lenti,[16] E.Leonardi,[36] P.Levtchenko,[37] C.Li,[20,18] E.Lieb,[45] W.T.Lin,[48] F.L.Linde,[2] B.Lindemann,[1] L.Lista,[28] Y.Liu,[18] Z.A.Liu,[6] W.Lohmann,[45] E.Longo,[36] W.Lu,[32] Y.S.Lu,[6] K.Lübelsmeyer,[1] C.Luci,[36] D.Luckey,[15] L.Ludovici,[36] L.Luminari,[36] W.Lustermann,[44] W.G.Ma,[20] A.Macchiolo,[16] M.Maity,[9] L.Malgeri,[36] R.Malik,[18] A.Malinin,[27] C.Maña,[25] S.Mangla,[9] M.Maolinbay,[46] P.Marchesini,[46] A.Marin,[10] J.P.Martin,[24] F.Marzano,[36] G.G.G.Massaro,[2] K.Mazumdar,[9] D.McNally,[17] S.Mele,[28] M.Merk,[34] L.Merola,[28] M.Meschini,[16] W.J.Metzger,[30] Y.Mi,[22] A.Mihul,[12] A.J.W.van Mil,[30] Y.Mir,[18] G.Mirabelli,[36] J.Mnich,[17] M.Möller,[1] V.Monaco,[36] B.Monteleoni,[16] R.Moore,[3] R.Morand,[4] S.Morganti,[36] N.E.Moulai,[18] R.Mount,[32] S.Müller,[1] E.Nagy,[13] S.Nahn,[15] M.Napolitano,[28] F.Nessi-Tedaldi,[46] H.Newman,[32] M.A.Niaz,[18] A.Nippe,[1] H.Nowak,[45] G.Organtini,[36] R.Ostonen,[21] D.Pandoulas,[1] S.Paoletti,[36] P.Paolucci,[28] G.Pascale,[36] G.Passaleva,[16] S.Patricelli,[28] T.Paul,[33] M.Pauluzzi,[33] C.Paus,[1] F.Pauss,[46] Y.J.Pei,[1] S.Pensotti,[26] D.Perret-Gallix,[4] A.Pevsner,[5] D.Piccolo,[28] M.Pieri,[16] J.C.Pinto,[34] P.A.Piroué,[35] E.Pistolesi,[16] V.Plyaskin,[27] M.Pohl,[46] V.Pojidaev,[27,16] H.Postema,[15] N.Produit,[19] K.N.Qureshi,[18] R.Raghavan,[9] G.Rahal-Callot,[46] P.G.Rancoita,[26] M.Rattaggi,[26] G.Raven,[2] P.Razis,[29] K.Read,[31] M.Redaelli,[26] D.Ren,[46] Z.Ren,[18] M.Rescigno,[36] S.Reucroft,[11] A.Ricker,[1] S.Riemann,[45] B.C.Riemers,[43] K.Riles,[3] O.Rind,[3] H.A.Rizvi,[18] S.Ro,[41] A.Robohm,[46] J.Rodin,[15] F.J.Rodriguez,[25] B.P.Roe,[3] M.Röhner,[1] S.Röhner,[1] L.Romero,[25] S.Rosier-Lees,[4] Ph.Rosselet,[22] W.van Rossum,[2] S.Roth,[1] J.A.Rubio,[17] H.Rykaczewski,[46] J.Salicio,[17] J.M.Salicio,[25] E.Sanchez,[25] A.Santocchia,[33] M.E.Sarakinos,[21] S.Sarkar,[9] G.Sartorelli,[18] M.Sassowsky,[1] G.Sauvage,[4] C.Schäfer,[1] V.Schegelsky,[37] D.Schmitz,[1] P.Schmitz,[1] M.Schneegans,[4] B.Schoeneich,[45] N.Scholz,[46] H.Schopper,[47] D.J.Schotanus,[30] R.Schulte,[1] K.Schultze,[1] J.Schwenke,[1] G.Schwering,[1] C.Sciacca,[28] R.Sehgal,[18] P.G.Seiler,[44] J.C.Sens,[48] L.Servoli,[33] S.Shevchenko,[32] N.Shivarov,[40] V.Shoutko,[27] J.Shukla,[23] E.Shumilov,[27] D.Son,[41] A.Sopczak,[17] V.Soulimov,[28] B.Smith,[15] T.Spickermann,[1] P.Spillantini,[16] M.Steuer,[15] D.P.Stickland,[35] F.Sticozzi,[15] H.Stone,[35] B.Stoyanov,[40] K.Strauch,[14] K.Sudhakar,[9] G.Sultanov,[18] L.Z.Sun,[20,18] G.F.Susinno,[19] H.Suter,[46] J.D.Swain,[18] A.A.Syed,[30] X.W.Tang,[6] L.Taylor,[11] R.Timellini,[8] Samuel C.C.Ting,[15] S.M.Ting,[15] O.Toker,[33] M.Tonutti,[1] S.C.Tonwar,[9] J.Tóth,[13] A.Tsaregorodtsev,[37] G.Tsipolitis,[34] C.Tully,[35] H.Tuchscherer,[42] J.Ulbricht,[46] L.Urbán,[13] U.Uwer,[1] E.Valente,[36] R.T.Van de Walle,[30] I.Vetlitsky,[27] G.Viertel,[46] P.Vikas,[18] U.Vikas,[18] M.Vivargent,[4] R.Voelkert,[45] H.Vogel,[34] H.Vogt,[45] I.Vorobiev,[27] A.A.Vorobyov,[37] An.A.Vorobyov,[37] L.Vuilleumier,[22] M.Wadhwa,[25] W.Wallraff,[1] J.C.Wang,[15] X.L.Wang,[20] Y.F.Wang,[15] Z.M.Wang,[18,20] A.Weber,[1] R.Weill,[22] C.Willmott,[25] F.Wittgenstein,[17] S.X.Wu,[18] S.Wynhoff,[1] J.Xu,[10] Z.Z.Xu,[20] B.Z.Yang,[20] C.G.Yang,[6] G.Yang,[18] X.Y.Yao,[6] C.H.Ye,[18] J.B.Ye,[20] Q.Ye,[18] S.C.Yeh,[48] J.M.You,[34] N.Yunus,[18] M.Yzerman,[2] C.Zaccardelli,[32] An.Zalite,[37] P.Zemp,[46] J.Y.Zeng,[6] M.Zeng,[18] Y.Zeng,[1] Z.Zhang,[6] Z.P.Zhang,[20,18] B.Zhou,[10] G.J.Zhou,[6] J.F.Zhou,[1] Y.Zhou,[3] G.Y.Zhu,[6] R.Y.Zhu,[32] A.Zichichi,[8,17,18] B.C.C.van der Zwaan.[2]

1 I. Physikalisches Institut, RWTH, D-52056 Aachen, FRG§
III. Physikalisches Institut, RWTH, D-52056 Aachen, FRG§
2 National Institute for High Energy Physics, NIKHEF, NL-1009 DB Amsterdam, The Netherlands
3 University of Michigan, Ann Arbor, MI 48109, USA
4 Laboratoire d'Annecy-le-Vieux de Physique des Particules, LAPP,IN2P3-CNRS, BP 110, F-74941 Annecy-le-Vieux CEDEX, France
5 Johns Hopkins University, Baltimore, MD 21218, USA
6 Institute of High Energy Physics, IHEP, 100039 Beijing, China
7 Humboldt University, D-10099 Berlin, FRG§
8 INFN-Sezione di Bologna, I-40126 Bologna, Italy
9 Tata Institute of Fundamental Research, Bombay 400 005, India
10 Boston University, Boston, MA 02215, USA
11 Northeastern University, Boston, MA 02115, USA
12 Institute of Atomic Physics and University of Bucharest, R-76900 Bucharest, Romania
13 Central Research Institute for Physics of the Hungarian Academy of Sciences, H-1525 Budapest 114, Hungary‡
14 Harvard University, Cambridge, MA 02139, USA
15 Massachusetts Institute of Technology, Cambridge, MA 02139, USA
16 INFN Sezione di Firenze and University of Florence, I-50125 Florence, Italy
17 European Laboratory for Particle Physics, CERN, CH-1211 Geneva 23, Switzerland
18 World Laboratory, FBLJA Project, CH-1211 Geneva 23, Switzerland
19 University of Geneva, CH-1211 Geneva 4, Switzerland
20 Chinese University of Science and Technology, USTC, Hefei, Anhui 230 029, China
21 SEFT, Research Institute for High Energy Physics, P.O. Box 9, SF-00014 Helsinki, Finland
22 University of Lausanne, CH-1015 Lausanne, Switzerland
23 Los Alamos National Laboratory, Los Alamos, NM 87544, USA
24 Institut de Physique Nucléaire de Lyon, IN2P3-CNRS,Université Claude Bernard, F-69622 Villeurbanne Cedex, France
25 Centro de Investigaciones Energeticas, Medioambientales y Tecnologicas, CIEMAT, E-28040 Madrid, Spain♭
26 INFN-Sezione di Milano, I-20133 Milan, Italy
27 Institute of Theoretical and Experimental Physics, ITEP, Moscow, Russia
28 INFN-Sezione di Napoli and University of Naples, I-80125 Naples, Italy
29 Department of Natural Sciences, University of Cyprus, Nicosia, Cyprus
30 University of Nymegen and NIKHEF, NL-6525 ED Nymegen, The Netherlands
31 Oak Ridge National Laboratory, Oak Ridge, TN 37831, USA
32 California Institute of Technology, Pasadena, CA 91125, USA
33 INFN-Sezione di Perugia and Universitá Degli Studi di Perugia, I-06100 Perugia, Italy
34 Carnegie Mellon University, Pittsburgh, PA 15213, USA
35 Princeton University, Princeton, NJ 08544, USA
36 INFN-Sezione di Roma and University of Rome, "La Sapienza", I-00185 Rome, Italy
37 Nuclear Physics Institute, St. Petersburg, Russia
38 University of California, San Diego, CA 92093, USA
39 Dept. de Fisica de Particulas Elementales, Univ. de Santiago, E-15706 Santiago de Compostela, Spain
40 Bulgarian Academy of Sciences, Central Laboratory of Mechatronics and Instrumentation, BU-1113 Sofia, Bulgaria
41 Center for High Energy Physics, Korea Advanced Inst. of Sciences and Technology, 305-701 Taejon, Republic of Korea
42 University of Alabama, Tuscaloosa, AL 35486, USA
43 Purdue University, West Lafayette, IN 47907, USA
44 Paul Scherrer Institut, PSI, CH-5232 Villigen, Switzerland
45 DESY-Institut für Hochenergiephysik, D-15738 Zeuthen, FRG
46 Eidgenössische Technische Hochschule, ETH Zürich, CH-8093 Zürich, Switzerland
47 University of Hamburg, D-22761 Hamburg, FRG
48 High Energy Physics Group, Taiwan, China
§ Supported by the German Bundesministerium für Bildung, Wissenschaft, Forschung und Technologie
‡ Supported by the Hungarian OTKA fund under contract number 2970.
♭ Supported also by the Comisión Interministerial de Ciencia y Technología
♮ Also supported by CONICET and Universidad Nacional de La Plata, CC 67, 1900 La Plata, Argentina

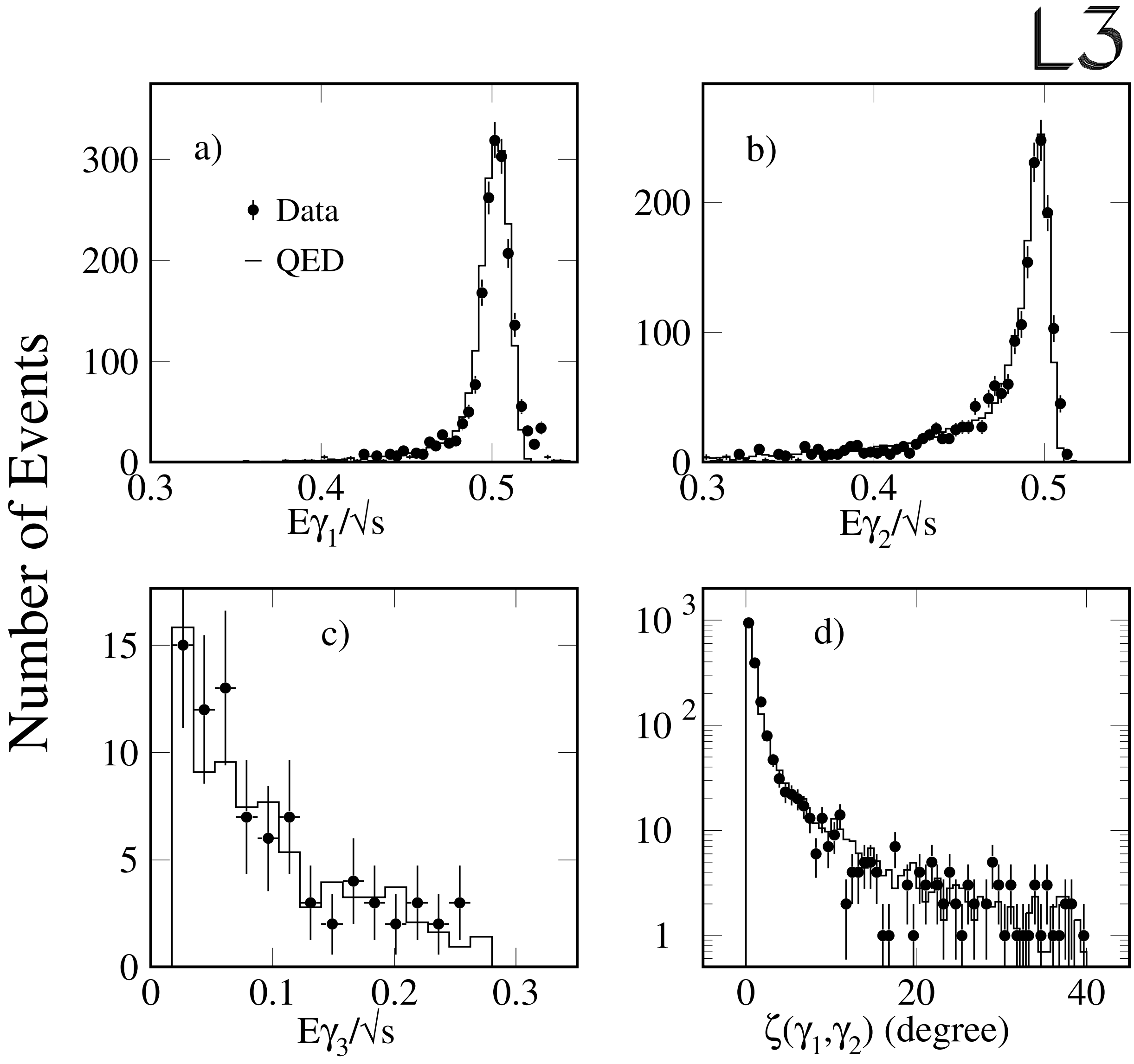

Figure 1: (a), (b) and (c) show the comparisons between the data and the QED predictions of the normalized photon energy spectra for the first, second and third most energetic photons, respectively. (d) shows the comparison of the acollinearity angle distribution between the two most energetic photons.

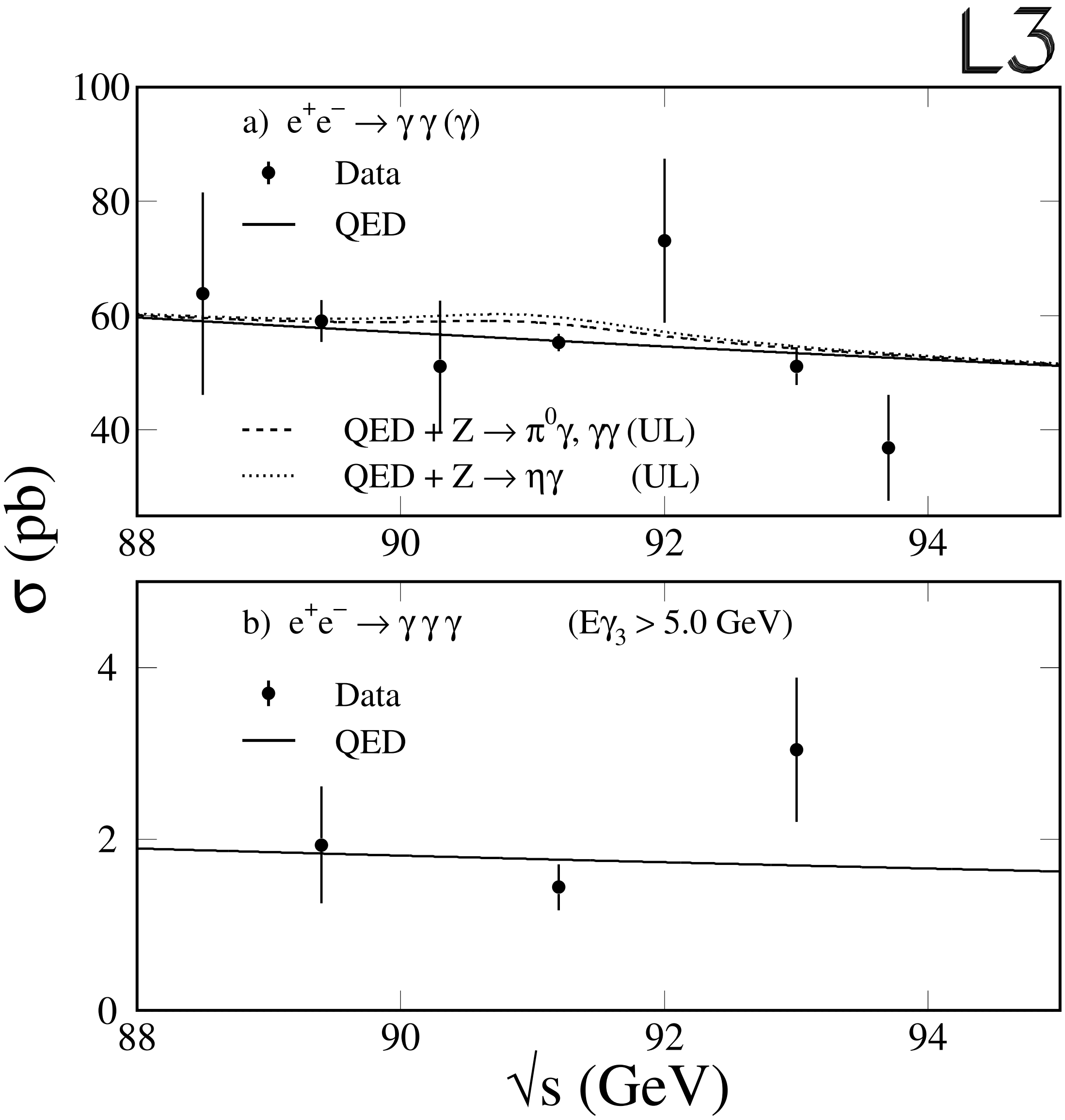

Figure 2: Comparison of the total cross sections between the data and the QED prediction as a function of center of mass energy. In (a) upper limits (UL), at 95% CL, on the rare and forbidden processes are also shown.

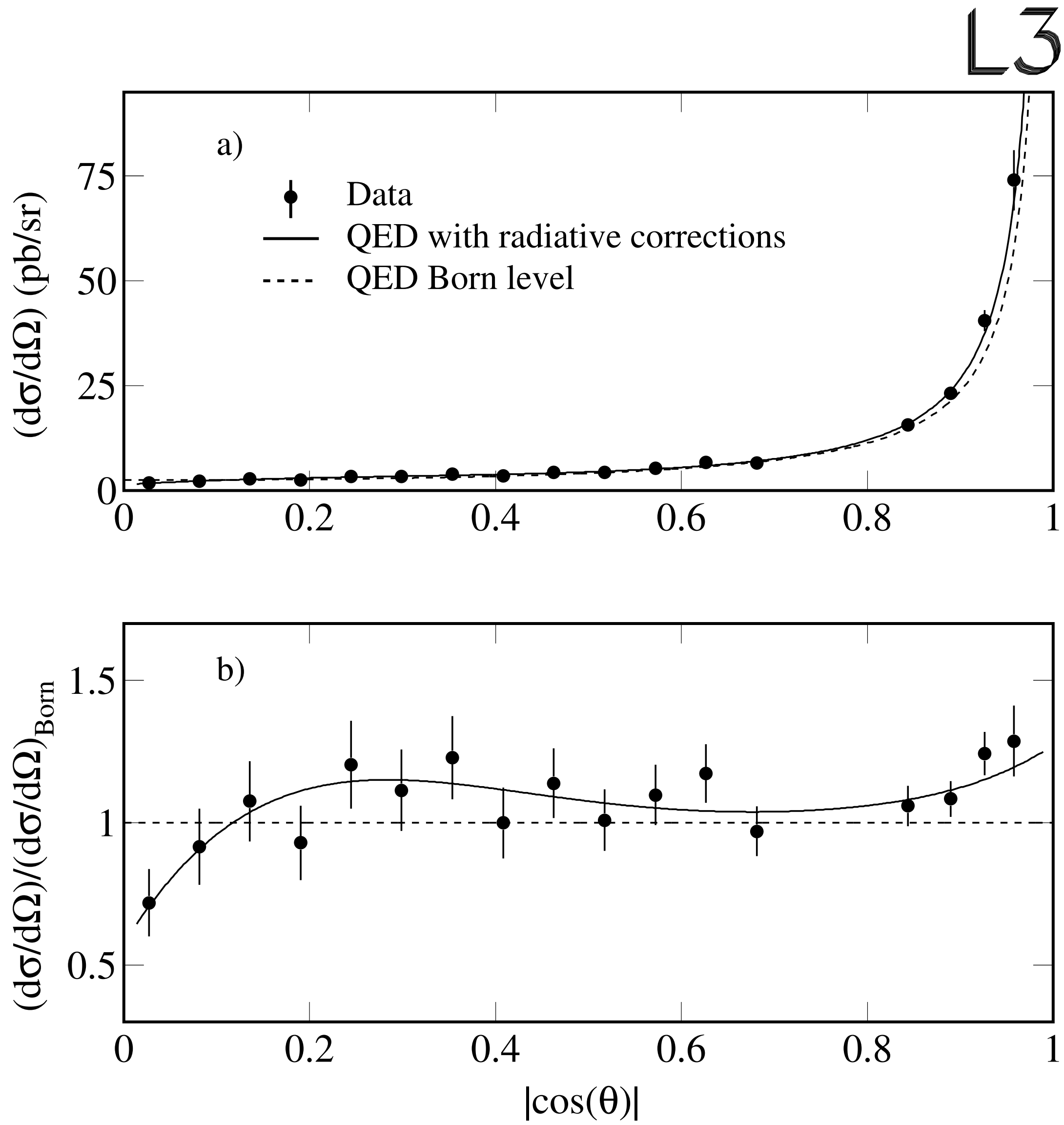

Figure 3: (a) shows the comparison of measured differential cross sections with the QED predictions for the process $e^+e^- \to \gamma\gamma(\gamma)$ as a function of $|\cos\theta|$. (b) shows the same cross sections normalized to the QED Born level prediction.

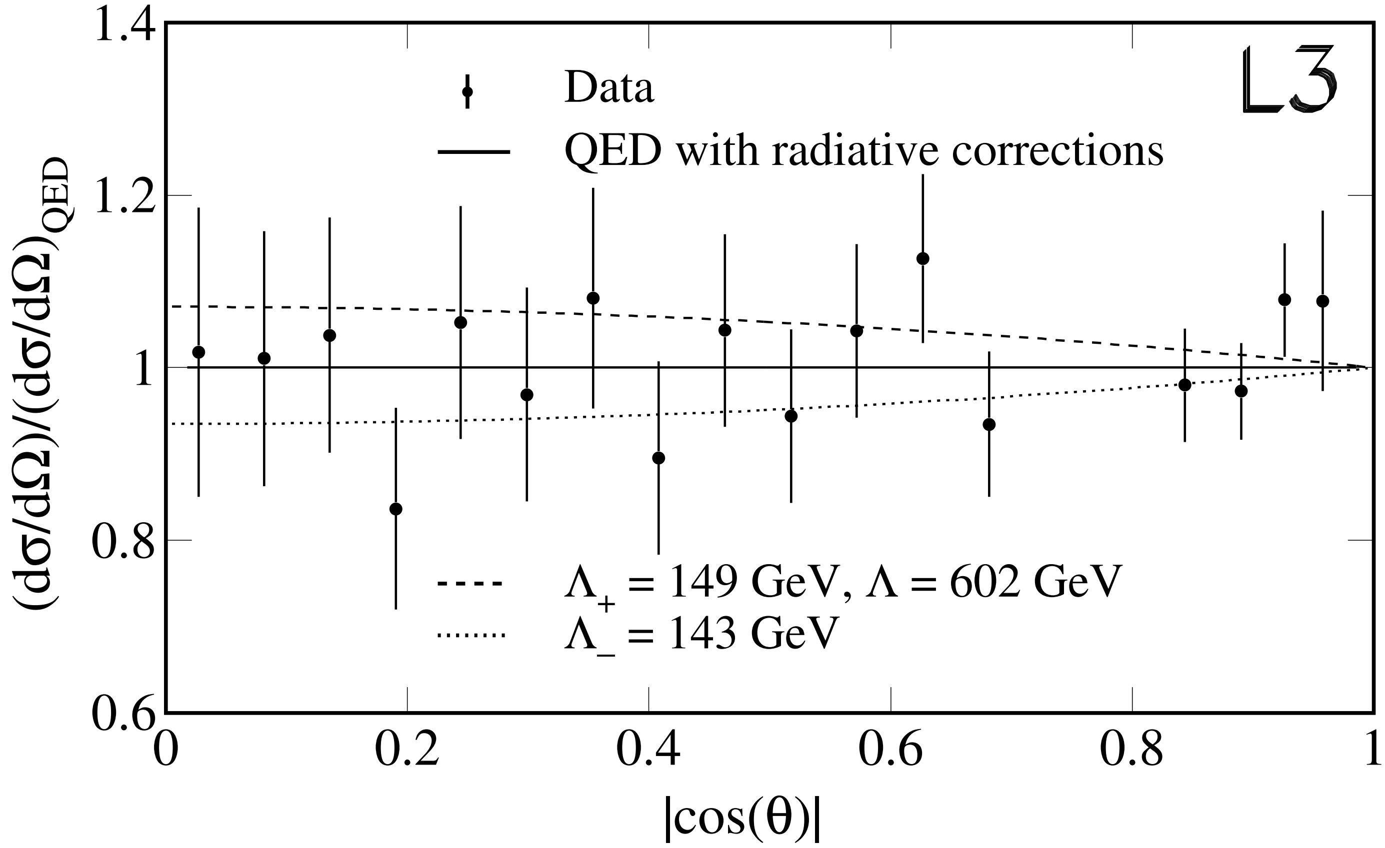

Figure 4: Comparison of the measured differential cross section with the QED predictions including the deviations for the parameter values shown in the figure, as a function of $|\cos\theta|$. The cross sections are normalized to the radiatively corrected QED cross section. The functional effect of Λ_+ and Λ is the same.

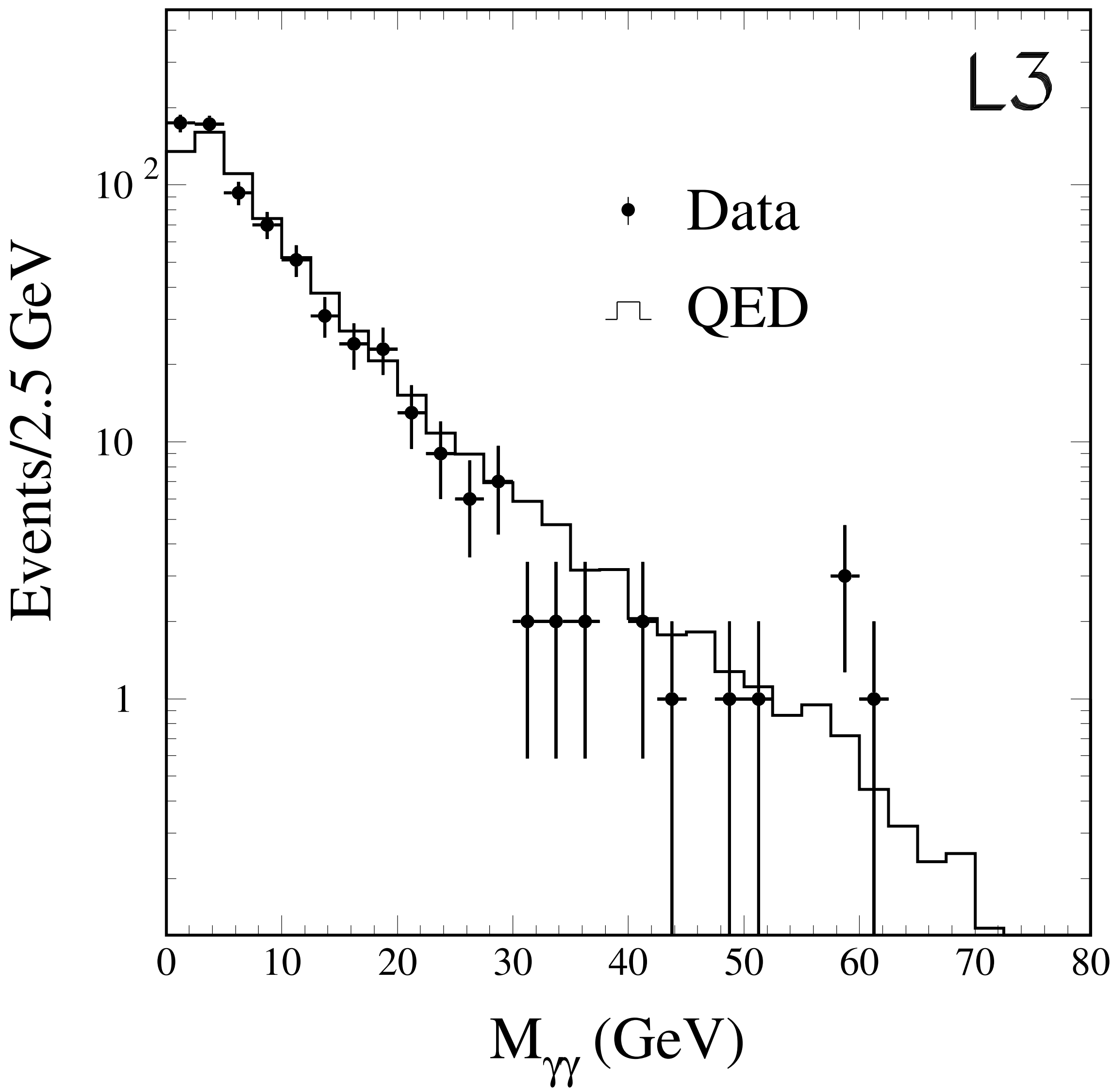

Figure 5: $\gamma\gamma$ invariant mass distribution compared to the QED predictions for the process $e^+e^- \to \ell^+\ell^-\gamma\gamma$.